Research Article Vol. 4, No. 3 / 15 March 2021 / OSA Continuum 783

Telecentric F-theta fisheye lens for space applications

CLAUDIO PERNECHELE,[1,*] LUCA CONSOLARO,[2] GERAINT H. JONES,[3,4] GEORGE BRYDON,[3,4] AND VANIA DA DEPPO[5]

[1]National Institute for Astrophysics, Padova, Vicolo dell'Osservatorio, 5, 35122 Padova, Italy
[2]Lobre srl, Via Meucci 6, 25013 Carpenedolo (Brescia), Italy
[3]UCL Mullard Space Science Laboratory, Holmbury St. Mary, Dorking RH5 6NT, UK
[4]The Centre for Planetary Sciences UCL/Birkbeck, Gower Street, London, WC1E 1BT, UK
[5]CNR-IFN Padova, Via Trasea 7, 35131 Padova, Italy
[*]claudio.pernechele@inaf.it

Abstract: A very wide angle lens with a field of view of 360°x180° - a fisheye lens - has been designed to be used in a space environment. As a case study, the lens is assumed to be mounted on a spinning probe passing through a comet's tail. The lens, rotating with the probe passing through the comet coma, may map the entire sky as viewed from the interior tail, providing unprecedented data on the spatial distribution of plasma and dust. Considering the foreseen space applications for the lens, radiation hardened glass has been taken into account for the design. A key feature of the lens is the "angular scale" uniformity (F-theta) of the sky distribution map projected on the focal plane allowing to obtain a reliable whole sky reconstruction. Care has also been taken to obtain an almost telecentric design, in order to permit filters placed on the focal plane to work properly. A telecentric fisheye operating with a pixel-limited resolution in the waveband from 500 nm up to 770 nm and with an F-theta distortion is presented in this paper.

1. Introduction

The fisheye is the paradigm for a very wide angle lens and these lenses have found some applications also in astronomical research. These lenses have been proposed for space-based observations of heliospheric features [1]; the solar mass ejection imager (SMEI) aboard the Coriolis spacecraft has been designed to detect and forecast the arrival of solar mass ejections [2]; the Mars Color Imager (MARCI) aboard the Mars Reconnaissance Orbiter spacecraft [3] use of fisheye optics; an explorative study for applying a hyper-hemispheric lens as a medium-resolution star tracker for mini- and micro-satellites has been published [4,5]; for ground based astronomy, fisheyes are used in all-sky photographic cameras to determine meteor trajectory [6]. In astronomical or, more generally, metrological applications of very wide angle lenses, an accurate determination on how the field of view is mapped into the focal plane is mandatory to obtain calibrated data, both for real/apparent orbit determination (astrometry) and flux/brightness calibration. Each application may need a different mapping function and the optical designer should bear this in mind in optimizing the proper fisheye layout.

The Entire Visible Sky (EnVisS) is one of the payloads [7] to be mounted on the ESA F-Class mission Comet Interceptor [8,9]. The main aim of the mission is the study of a dynamically new comet – i.e. a comet that never traveled through the solar system - or an interstellar object, entering the inner solar system. The EnVisS camera's aim is to capture the entire sky in the 500-770 nm wavelength band while the spacecraft passes through the comet's tail environment. To consider a realistic scenario, the EnVisS instrument has been used as a case study to design a space grade fisheye objective with a field of view of 360° x 180° coupled with a commercial off-the-shelf (COTS) imaging detector.

#412566 https://doi.org/10.1364/OSAC.412566
Journal © 2021 Received 29 Oct 2020; revised 11 Dec 2020; accepted 11 Dec 2020; published 18 Feb 2021

OSA CONTINUUM

In this paper a fisheye lens with an equidistant (F-theta) sky mapping function and a pixel limited performance is described and discussed. F-theta design is important to maintain low the distortion, facilitating image analysis. Telecentric design will assure that eventual filters placed in the focal plane will work properly at every field (the waveband may change with the rays' arrival angles).

2. Fisheye optical design

A very wide angle lens, as is a fisheye, must provide a distorted image in order to fit a finite-sized imaging detector. This distortion is introduced by the optical designer depending on the desired applications. Each possible distortion function has a different field of view map and this must be taken into account by the scientific/metrological user, because the plate scale results are variable along the focal plane. To obtain useful scientific information from fisheye images (astrometry, flux calibration and brightness measurements), the mapping function has to be accurately determined. In this paper we design a fisheye with an equidistant distortion map. The design of very wide angle lenses requires accounting for some typical issues. The fundamental origin of the optical problem resides in the entrance pupil shift at large field angles, where the paraxial approximation is no longer valid: chief ray angles on the object side are not preserved passing through the optics preceding the aperture stop (fore-optics). This effect produces an image deformation, with the focal length changing along the elevation angles. When the zenith (or field) angle becomes wide, the aperture stop is seen slanting and, at the limit angle of 90°, it will result in becoming completely obstructed. In order to permit the visibility of objects at high Z fields, the entrance pupil should be tilted. This movement is possible at the cost of some pupil compression, which alters the exit pupil flux.

2.1. Fisheye optical layout

We designed a fisheye lens based on a COTS monochrome image sensor with a format of $2k^2$ pixels with a 5.5 µm squared pixel size. This has led to a fisheye focal length of 3.3 mm working at a relative aperture F/3. A ray-trace diagram of the lens' layout is shown in Fig. 1 (A.S. label shows the diaphragm position); parameters are listed in Table 1. The total track of the lens is 110 mm, while the frontal lens is 70 mm in diameter. Care has been taken on setting the first two lenses made of a radiation tolerant glass. Optical performance, in terms of polychromatic MTF and of spot size, are shown, respectively, in Figs. 2 and 3. The design result comparable with the pixel dimension (5.5 µm). The chief rays' angles of arrival are maintained within 4° along the entire field (telecentric condition).

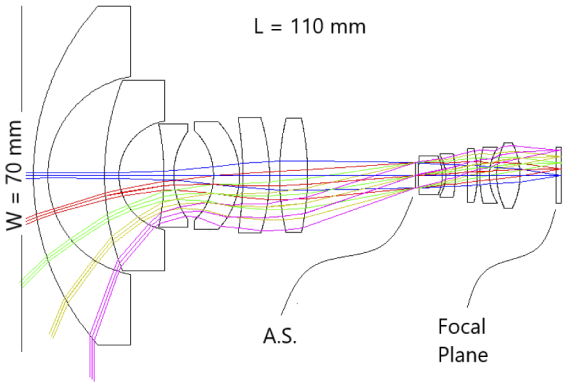

Fig. 1. Optical layout of the fisheye lens.

OSA CONTINUUM

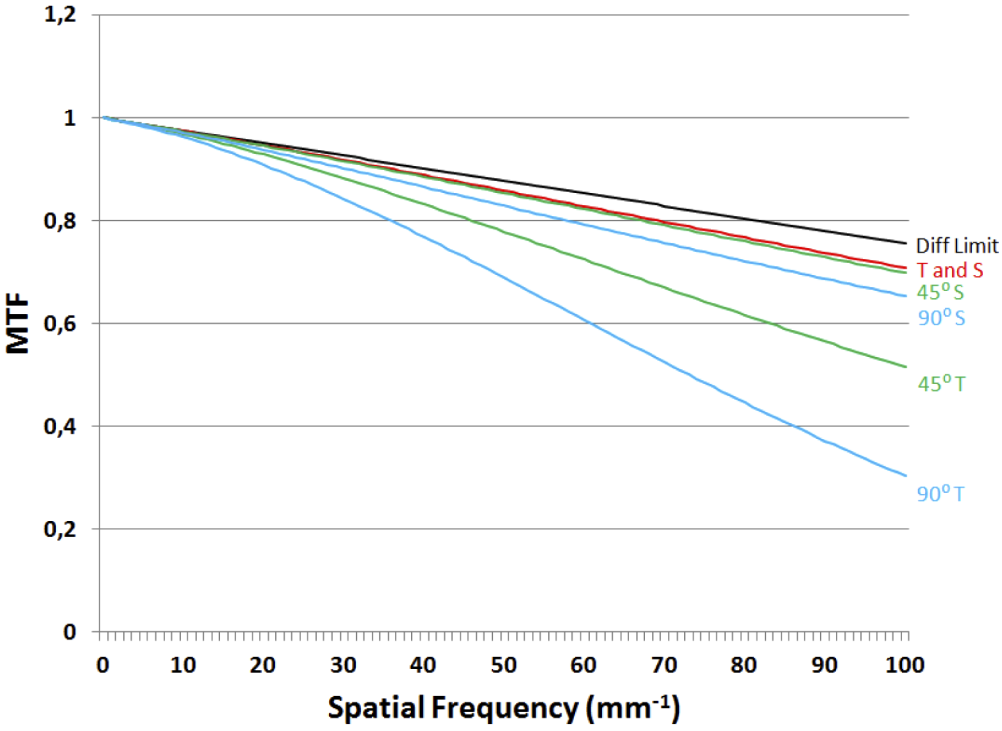

Fig. 2. MTF of the fisheye lens.

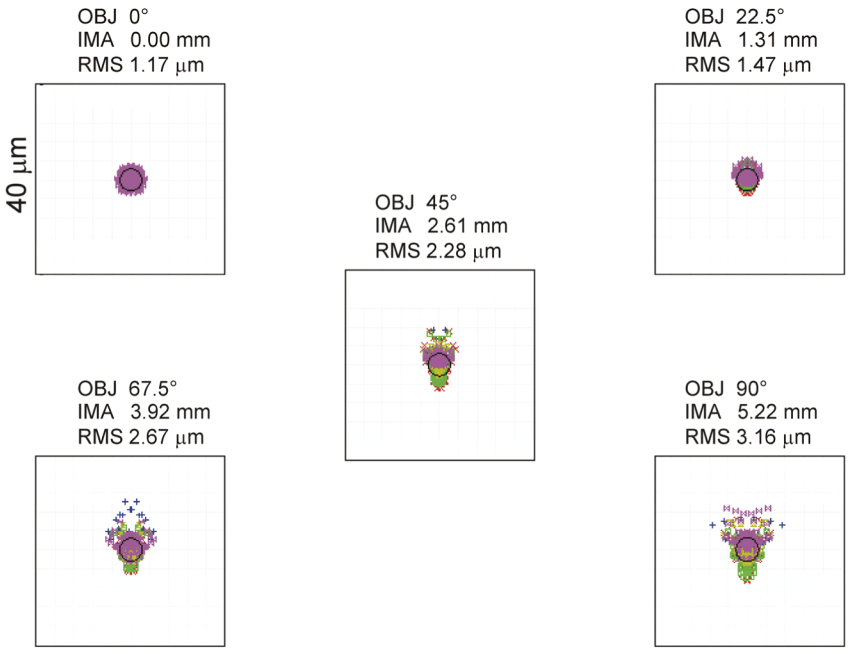

Fig. 3. Polychromatic (500-770 nm) spot diagrams of the fisheye lens. Shown diffraction limit circle is 2.32 µm.

OSA CONTINUUM

Table 1. Fisheye lens optical main parameters

Lens #	Thickness (mm)	Radius (mm)	Glass type	Diameter (mm)
1	3.00	52.46	K5G20	70
	11.70	20.78		
2	3.00	53.90	K5G20	40
	9.33	11.42		
3	2.00	-51.96	LAM73	20
	8.30	15.54		
4	5.35	-12.88	LAL14	22
	0.72	-16.21		
5	5.52	-70.96	LASF51	24
	2.10	-40.03		
6	5.80	52.50	LAK8	24
	22.43	-55.50		
A.S.	0.54	–	–	5.2
7	5.00	30.60	PSK53A	8
	0.70	-9.28		
8	2.00	-7.88	LAH58	9
	2.56	-24.94		
9	2.00	222.61	BSM4	11
	0.50	-20.71		
10	2.00	25.97	NPH3	12
	1.50	10.77		
11	4.83	14.81	PHM52	14
	7.50	-15.15		
window	1.00	Flat	Fused Silica	12

2.2. *Fisheye mapping function*

Referring to the top panel of Fig. 4, let be define R the radial distance of a chief ray field form the optical axis (ψ being its angular coordinate) and Z the angular field distance from the zenith. There are many ways in which the field (Z angles) may be mapped onto the focal plane, i.e. $R = R(Z)$. A "perfect" undistorted map of the object space is one where $\psi = Z$, i.e. $R = f \cdot tan(Z)$ with f the lens focal length. Every point in the space is mapped maintaining the same angular distribution into the focal plane and object straight lines remain straight (distortion free) in the image. This function is known as *perspective projection* and has no meaning for wide zenith angles, because the focal plane would be infinitely wide and the entrance pupil (the pin-hole) would be completely obscured at $Z = 90°$. In order to have a wide-angle lens useful for any application, some image distortion has to be introduced. *Equidistant* (also called F-theta or linear scaled) projection has the form $R = f \cdot Z$. The equidistant function maintains angular distances. The most generic mapping function is defined as $R = f \cdot k_1 \cdot \sin(k_2 \cdot Z)$, where k_1 and k_2 are dimensionless coefficients. One traditional and useful projection scheme is the *equisolid* angle projection (with $k_1 = 2$, $k_2 = 0.5$), which maintains surface relations. Each pixel in the detector subtends an equal solid angle, i.e. an equal area on the unit sphere. In the orthographic projection, also known as *sine-law* projection ($k_1 = k_2 = 1$), the focal plane radial distribution is $R = f \cdot sin(Z)$. This projection maintains planar illuminance and the marginal fields are extremely compressed at the focal plane. Our F-theta lens distortion (deviation from linearity) is plotted in the bottom panel of Fig. 4.

OSA CONTINUUM

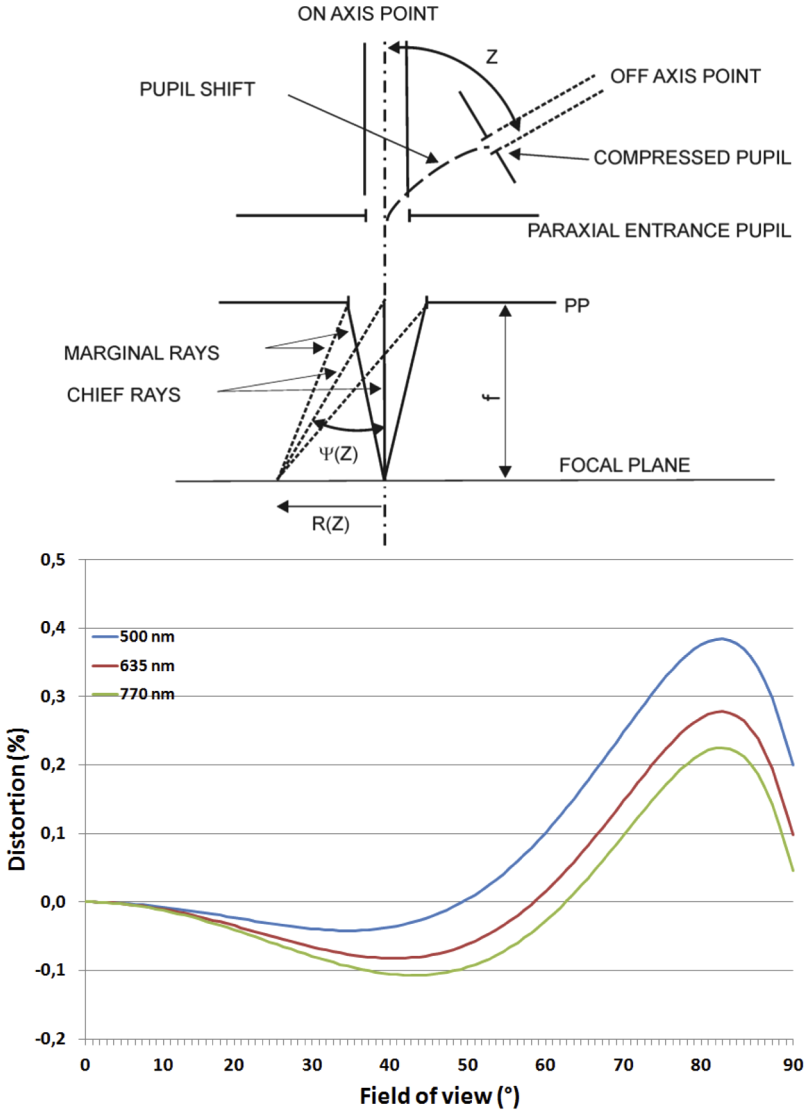

Fig. 4. Image formation in a very wide angle lens (top) and actual F-theta fisheye distortion (bottom).

2.3. *Fisheye plate scale*

The difference in values between the spatial resolution along the zenith (Z) and azimuth (AZ) axes reflects the anamorphism of the fisheye lens. We designed a fisheye with an equidistant linear-scaled projection scheme ($R/f = Z$), then the plate scales (mm^{-1}) and the resolution (°/px) is summarized in the following relations (considering a 2kx2k sensor, see Ref. [4] for details):

$$RES_Z = \frac{\partial Z}{\partial R} = \frac{1}{f} \ mm^{-1} \rightarrow 0.09 \qquad ^\circ/px$$

$$RES_{AZ} = \frac{1}{f}\frac{\sin(Z)}{Z} \ mm^{-1} \rightarrow \frac{360^\circ \ \sin(Z)}{2\pi R_{PX}} \qquad ^\circ/px$$

OSA CONTINUUM

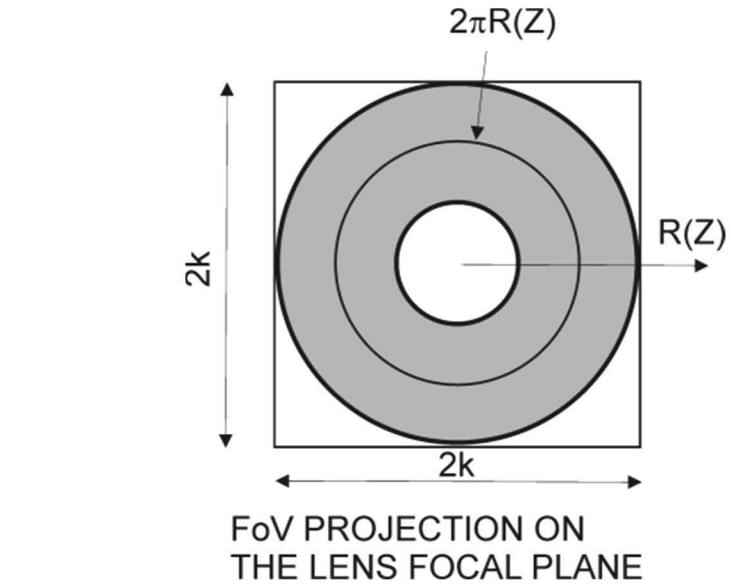

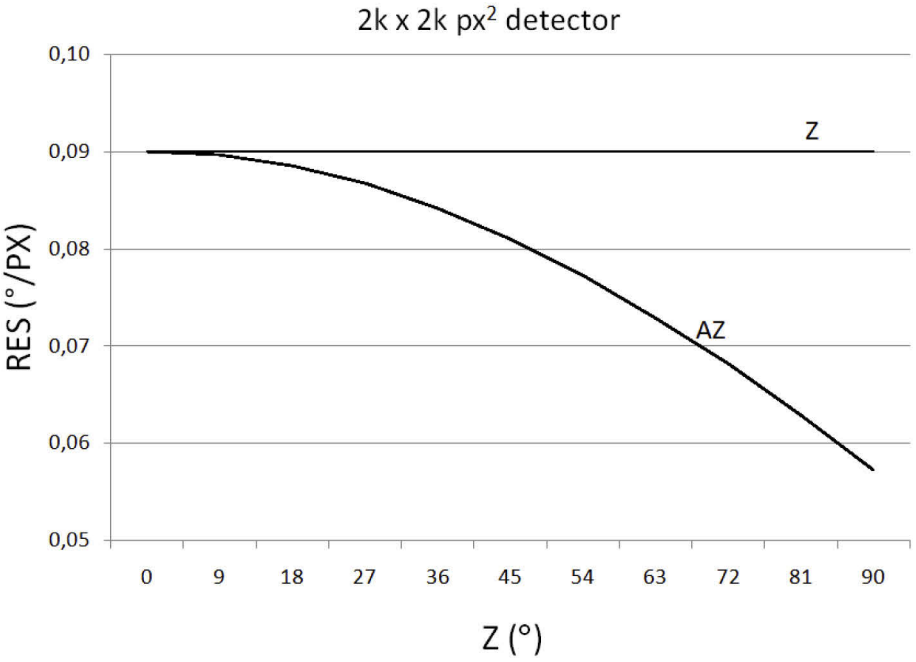

Fig. 5. Z and AZ image forming (top) and resolution (°/px) of the lens considering a 2k x 2k image sensor (bottom).

OSA CONTINUUM

RES_Z and RES_{AZ} are the resolutions (degrees/px) along elevation and azimuth axes. R_{PX} is the radius of a given azimuth circle projected in the focal plane, expressed in pixel units. The resolution is constant along the elevation axis (by construction), while along the AZ axis it increases with Z (RES_{AZ} is not defined for $R_{PX}=0$). Indeed, the length of the projected circumference is $2\pi R$ (see Fig. 5, top panel), while the on-sky angular value is $AZ=360°sin(Z)$. The AZ resolution is plotted in the bottom panel of Fig. 5 and, as expected, the resolution becomes finer as Z increases, i.e. the length of the projected circumference grows faster than the $AZ(Z)$ values. R_{PX} is the projected circumference radius (R) expressed in pixel units.

The instantaneous field view as viewed from a detector pixel is:

$$IFoV = \frac{1}{f}\Delta px \cdot \frac{1}{f}\frac{\sin(Z)}{Z}\Delta px$$

with Δpx the (squared) pixel dimension and f the lens focal length (3.3 mm in our case). The multiplication factors are maintained separately to underline the lens' anamorphism: the plate scales are different along Z and AZ axes. The instantaneous field of view is different along the Z (the former factor, independent by the Z angles) and AZ (the second one, variable with Z) axes. Given $[sin((Z)/Z] \leq 1$, the pixel resolution along AZ becomes finest approaching the horizon.

3. Conclusion

A fisheye for space applications has been designed. Care has been taken in selecting radiation tolerant glass and in having an equidistant (F-theta) sky mapping function. As a case study has been chosen the ESA F-class mission Comet Interceptor's EnVisS camera. This paper shows a fisheye optical design with marginal chief-ray impact angle which deviates from the telecentric condition by 4° and an F-theta distortion lower than 0.5%.

Funding. Agenzia Spaziale Italiana (2020-4-HH.0).

Acknowledgements. GHJ is grateful to the UK Space Agency for support. GB is supported by a UK Science and Technology Facilities Council (STFC) PhD studentship.

Disclosures. The author declare no conflicts of interest.

References

1. A. Buffington, P. P. Hick, B. V. Jackson, and C. M. Korendyke, "Corrals, hubcaps and crystal balls: some new design for very-wide-angle visible-light heliospheric imagers," Proc. SPIE **3442**, 77–86 (1998).
2. C. J. Eyles, G. M. Simnett, M. P. Cooke, B. V. Jackson, A. Buffington, P. P. Hick, N. R. Waltham, J. M. King, P. A. Anderson, and P. E. Holladay, "The Solar Mass Ejection Imager (SMEI)," Sol. Phys. **217**(2), 319–347 (2003).
3. J. F. Bell III, J. Wolff, M. C. Calvin, B. A. Cantor, M. A. Caplinger, R. T. Clancy, K. S. Edgett, L. J. Edwards, J. Fahle, F. Ghaemi, R. M. Haberle, A. Hale, P. B. James, S. W. Lee, T. McConnochie, E. Noe Dobrea, M. A. Ravine, D. Schaeffer, K. D. Supulver, and P. C. Thomas, "Mars Reconnaissance Orbiter Mars Color Imager (MARCI): Instrument description, calibration and performance," J. Geophys. Res.: Planets **114**(E8), 2008JE003315 (2009).
4. C. Pernechele, C. Dionisio, M. Munari, R. Opromolla, G. Rufino, G. Fasano, M. Grassi, and S. Pastore, "Hyper hemispheric lens applications in small and micro satellites," Adv. Space Res. **62**(12), 3449–3461 (2018).
5. R. Opromolla, G. Fasano, G. Rufino, M. Grassi, C. Pernechele, and C. Dionisio, "A new star tracker concept for satellite attitude determination based on a multi-purpose panoramic camera," Acta Astronaut. **140**, 166–175 (2017).
6. J. Borovička, P. Spurný, and J. Keclíková, "A new positional astrometric method for all-sky cameras," A&ASS **112**, 173–178 (1995).
7. G. Brydon and G. H. Jones, "Comet Interceptor's EnVisS Camera: Multispectral and Polarimetric Full-sky Imager for a Comet Flyby," EPSC-DPS Meeting **13**, 1 (2019).
8. C. Snodgras and G. H. Jones, "The European Space Agency's Comet Interceptor lies in wait," Nat. Commun. **10**(1), 5418 (2019).
9. G. H. Jones and C Snodgras., "Comet Interceptor: a mission to an ancient world," *51th Lunar and Planetary Conference*, Woodlands, Texas (US), #2326, id. 2938, (2020).